Lysosomal Biogenesis and Implications for Hydroxychloroquine Disposition

Keagan P Collins, Sandra Witta, Jonathan W Coy, Yi Pang, Daniel L Gustafson

Colorado State University

Affiliations:

School of Biomedical Engineering; Colorado State University; Fort Collins, CO USA (KPC, SW, DLG); Department of Clinical Sciences; Colorado State University; Fort Collins, CO USA (DLG, JWC); University of Colorado Cancer Center; Anschutz Medical Campus; Aurora, CO USA (DLG); University of Akron; Department of Chemistry; Akron, OH USA (YP)

Journal of Pharmacology and Experimental Therapeutics - JPET-AR-2020-000309

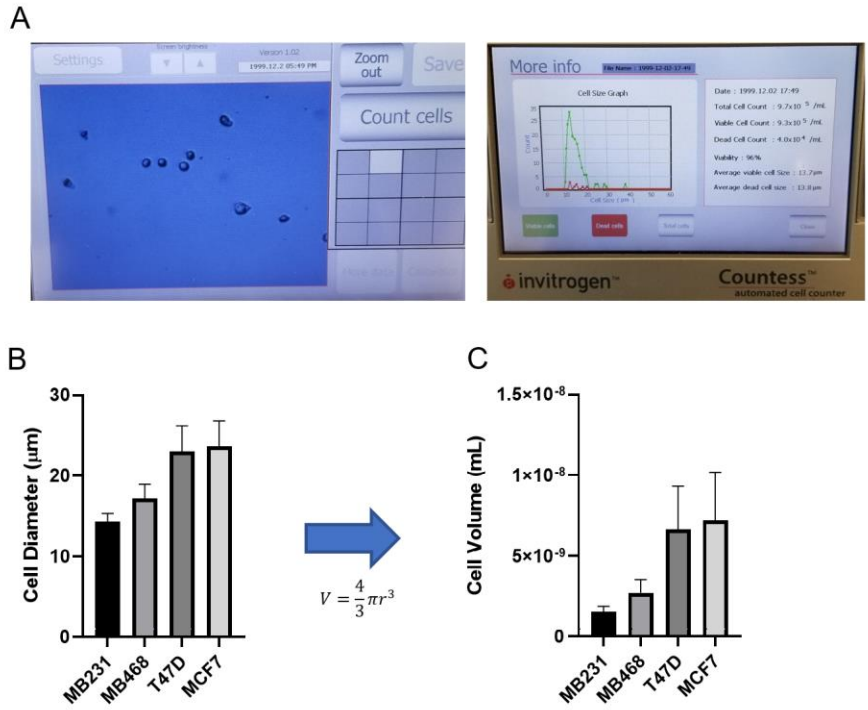

Supplementary Figure 1. Calculation of cell volumes
Volume for each cell line was determined by staining with live cell marker Trypan Blue, and then imaging suspended cells on a Countess Cell Counter System (A). Live cell diameter was determined by the mean cell diameter from 4 replicates (B). Cell volume was then calculated from the diameter for each cell line by assuming suspended cells were spherical (C). The geometric mean of the cell volume for each cell line was used in simulation. Data is presented as mean ± sd.

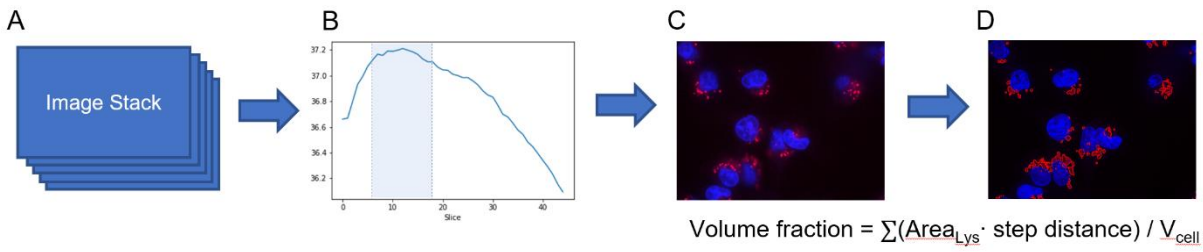

Supplementary Figure 2. Calculation of lysosomal volume fractions
Lysosome volume fraction of each cell line was determined by in-house macro methods. Live cells were treated with 1µM ETP for 30 minutes, followed by 10µM Hoechst 33342 for 10 minutes, and then imaging at 60x oil immersion confocal microscopy. 5-10 image stacks were taken per replicate at a step-size of 0.24µm, and 43 slices were taken per image stack on DAPI and Cy3 channels (A). Raw confocal image stacks were converted to .tif files and imported into Python version 3.7.6. Each slice of each image stack was analyzed to determine the peak signal to noise ratio (PSNR) using the sewar module (https://pypi.org/project/sewar/), and the top 10 slices were used for analysis (B). A FIJI macro that calculated the Cy3 (lysosome) area for each raw .vsi image slice based on an algebraic threshold of mean intensity was applied to raw images (C) to generate a lysosome area per slice, which is visualized in (D). Volume fraction for cells was calculated using the following equation: Volume fraction = $\sum(Area_{Lys} \cdot \text{step distance}) / V_{cell}$

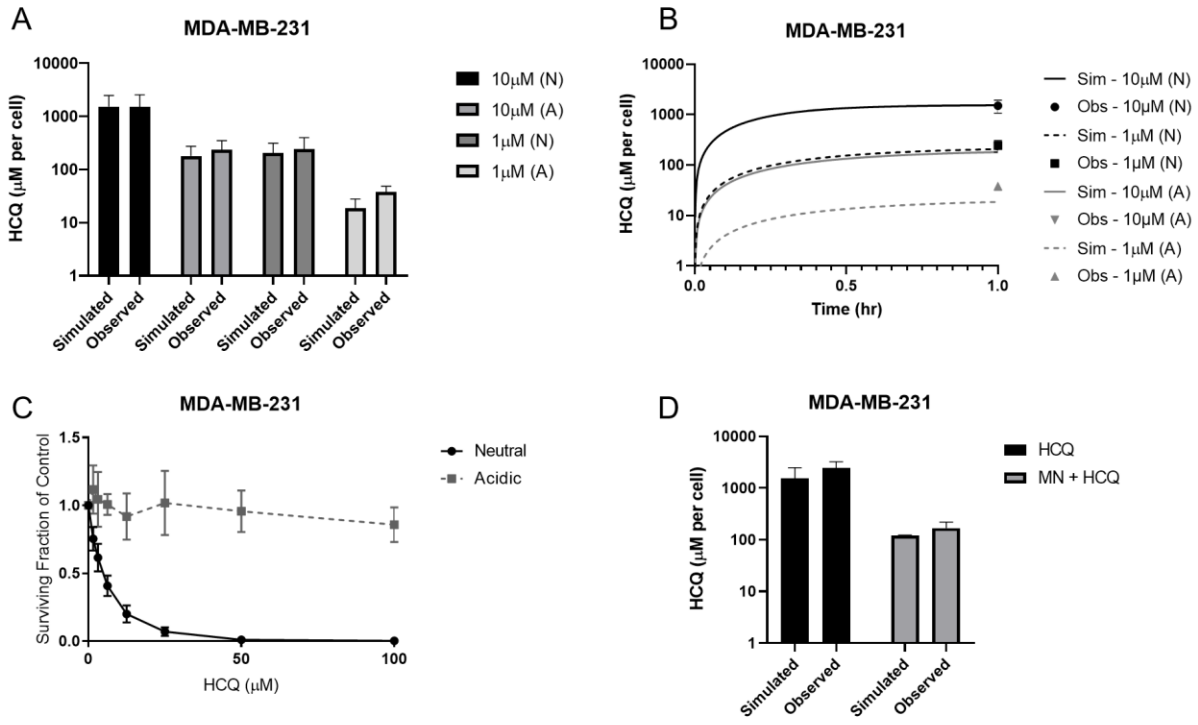

Supplementary Figure 3. Static PK Model Accounts for Variability Introduced by Modifying pH Parameters

To further investigate the capability of the model to simulate HCQ PK, we experimentally tested pH parameters within the model to compare to simulation data. We first investigated HCQ whole cell uptake at 1hr in MDA-MB-231 cells at pH_e of 7.6 (N) and 7.0 (A) at 1μM and 10μM for 1 hour and compared to simulation prediction in this cell line (A). The kinetic uptake curve was not visibly altered between pH_e or concentrations of HCQ μM (B). MDA-MB-231 growth inhibition was almost completely blunted in the presence of the acidic vs. neutral pH after 96hr of exposure (C). The role of the lysosome/cytosol pH gradient in MDA-MB-231 cells by pretreating cells with 25μM monensin (MN) for 30 minutes prior to adding 10μM HCQ for 1 hr (D).

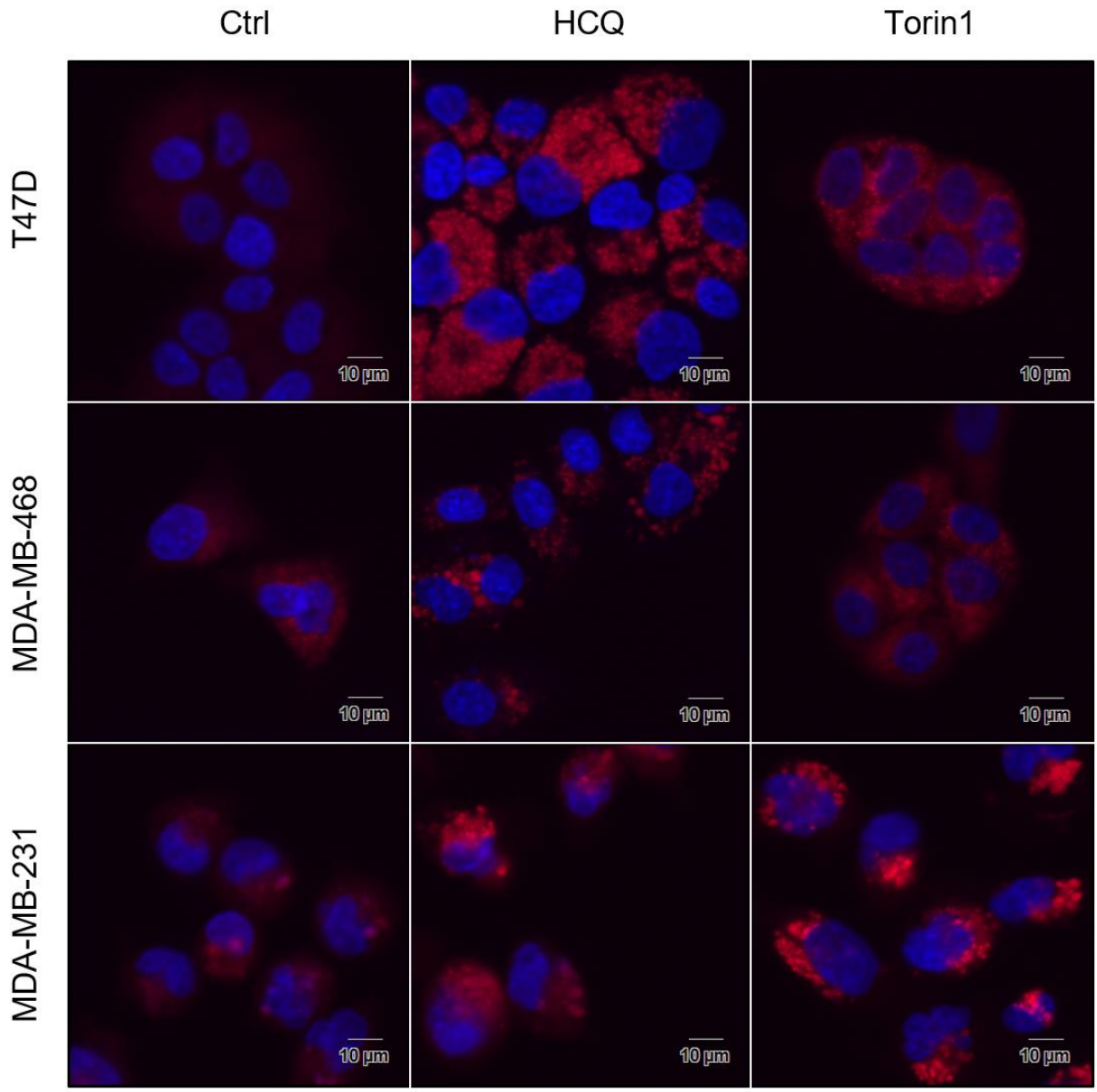

Supplementary Figure 4. HCQ and Torin1 treatment causes an increase in lysosomes within the cell

Representative images of T47D (top), MDA-MB-468 (center), and MDA-MB-231 (bottom) imaged with ETP after treatment with HCQ (center) or Torin 1 (right). An increase in lysosomes was visually apparent in all 3 cell lines (in addition to MCF7 – Figure 3) after both treatments. All cell lines appeared to have visibly larger lysosomes in HCQ treated vs. Torin 1 treated images. To prepare figures for publication the raw images threshold was adjusted to the same upper and lower bounds across the entire image for all images shown.

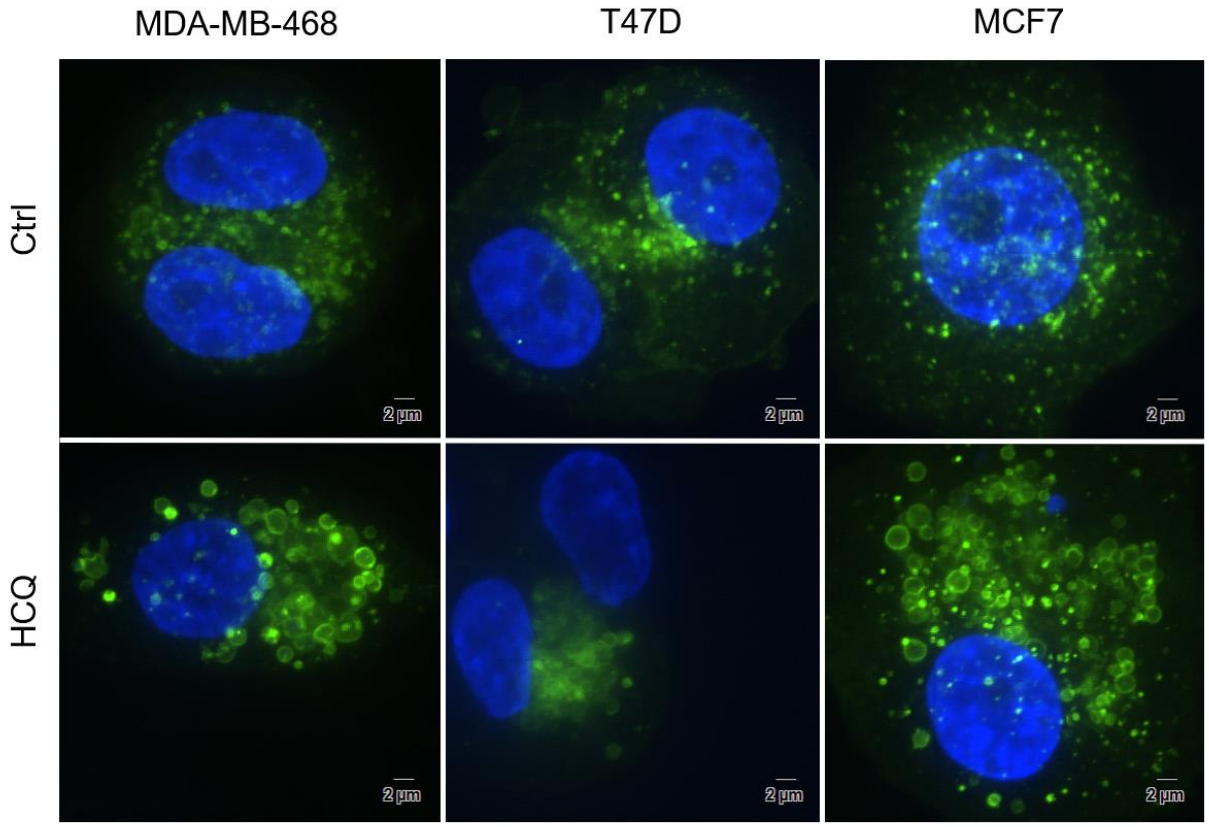

Supplementary Figure 5. HCQ treatment causes lysosomal swelling
MDA-MB-468 (left), T47D (center), and MCF7 (right) cells were transfected with GFP-LAMP-1 BacMam and treated with 10µM HCQ for 24 hours. Control cell lines (top) were observed to have LAMP-1 positive (lysosomes) vesicles appearing as small puncta located in the perinuclear region. HCQ treated cells (bottom) were all observed to have lysosomes that were much larger with much more defined membrane edges, though some smaller puncta were still present. To prepare images for publication, the 43-slice image stack was consolidated into a single image using EFI processing on Olympus CellSens software. All images were put through a sharpen filter, and then the GFP threshold was adjusted to the same upper and lower bounds across the entire image for all images shown.

Table S1. Model Parameters

Parameter	Symbol	Value
Global Model Parameters		
Molecular weight	MW	335.872
Lipophilicity[b]	Log P	3.84
First dissociation constant[b]	pKa_1	9.67
Second dissociation constant[b]	pKa_2	8.27
Lysosomal lipid fraction[a]	L	0.05
Lysosomal water fraction[a]	W	0.95
Neutral activity coefficient[a]	γ_N	1.23
First activity coefficient[a]	γ_1	0.74
Second activity coefficient[a]	γ_2	0.3
Lysosomal radius[a]	r_{lys}	0.275 (µm)
Lysosomal buffering capacity[a]	β	46,000 (µM)
Lysosomal pH[a]	pH_{lys}	5.0
Cytosolic pH[a]	pH_{cyt}	7.0
Extracellular pH[c]	pH_e	7.6
Lysosomal Volume Fractions	Vf_{lys}	%cell volume
MDA-MB-231[c]		3.67
MDA-MB-468[c]		1.41
T47D[c]		0.78
MCF7[c]		0.50

Footnotes:

[a]*Values from base model by Kornhuber et al. (2010)*

[b]*Values from Warhurst et al. (2003)*

[c]*Values determined experimentally*

Table S2. Static Model Metrics (Performance Error)

PE				
Time (min)	MDA-MB-231	MDA-MB-468	T47D	MCF7
1	66.87	79.32	33.48	-4.25
5	67.39	55.66	75.99	2.59
15	18.40	-1.33	39.15	-5.60
30	1.26	-7.03	64.00	-1.32
60	8.69	8.60	96.67	18.85
MAPE%				
	32.52	30.39	61.86	6.52
MPE%				
	18.40	8.60	64.00	-1.32

Table S3. Dynamic Model Metrics (Performance Error)

PE						
Time (min)	MDA-MB-231	MDA-MB-468	T47D	T47D (*2.5x*)	MCF7	MCF7 (*lower*)
1	83.92	95.30	45.79	43.98	4.41	4.41
5	63.99	53.02	72.25	52.47	1.27	1.39
15	18.15	-1.70	32.84	10.78	-6.81	-6.06
30	0.61	-8.04	44.13	22.85	-4.91	-2.70
60	6.79	5.70	46.42	40.78	8.81	14.87
240	30.59	20.14	3.27	65.13	-2.86	18.86
1440	11.71	25.73	-71.80	-2.67	-46.86	-4.40
MAPE%						
	30.82	29.95	45.21	34.09	10.85	7.53
MPE%						
	18.15	20.14	44.13	40.78	-2.86	1.39

Table S4. TFEB Dynamic Model Metrics (Performance Error)

PE	MB231	MB231	MB468	MB468	T47D	T47D (mean)	T47D (realistic)	MCF7	MCF7 (mean)	MCF7 (lower)
Time (min)	Ctrl	T1	Ctrl	T1	Ctrl	T1	T1	Ctrl	T1	T1
1	162.70	185.10	-9.74	57.73	25.14	-26.10	-17.79	36.21	32.59	37.27
5	72.71	120.40	-9.02	5.08	17.31	-44.83	-20.05	18.75	-25.25	-9.94
15	31.57	44.72	-10.32	-46.64	-14.7	-62.92	-37.21	1.63	-53.05	-37.93
30	18.39	-2.56	-3.07	-35.37	7.16	-70.79	-40.72	-0.05	-57.43	-38.56
60	20.46	-11.58	8.06	-33.54	6.05	-74.92	-34.68	16.18	-66.69	-47.61
240	35.25	4.05	46.56	-33.83	31.00	-74.74	-21.75	47.18	-54.27	-26.03
1440	8.17	6.65	41.57	24.13	6.98	-77.51	-31.81	10.56	-57.33	-30.29
MAPE%										
	49.89	53.58	18.33	33.76	15.48	61.69	29.14	18.65	49.52	32.52
MPE%										
	31.57	6.65	-3.07	-33.54	7.16	-70.79	-31.81	16.18	-54.27	-30.29